

Supplementary information

More Efficient Complement Activation by Anti-Aquaporin-4 Compared With Anti-Myelin Oligodendrocyte Glycoprotein Antibodies

Magdalena Lerch¹, MSc, Kathrin Schanda¹, MSc, Elliott Lafon², MSc, Reinhard Würzner², MD, PhD, Sara Mariotto³, MD, PhD, Alessandro Dinoto³, MD, Eva-Maria Wendel⁴, MD, Christian Lechner^{5,8}, MD, Harald Hegen¹, MD, PhD, Kevin Rostasy⁶, MD, Thomas Berger⁷, MD, Doris Wilflingseder², PhD, Romana Höftberger⁸, MD, Markus Reindl^{1#}, PhD

¹ Clinical Department of Neurology, Medical University of Innsbruck, Innsbruck, Austria

² Institute of Hygiene and Medical Microbiology, Medical University of Innsbruck, Innsbruck, Austria

³ Neurology Unit, Department of Neuroscience, Biomedicine, and Movement Sciences, University of Verona, Verona, Italy

⁴ Department of Pediatric Neurology, Olgahospital/Klinikum Stuttgart, Stuttgart, Germany

⁵ Department of Pediatrics I, Medical University of Innsbruck, Innsbruck, Austria

⁶ Paediatric Neurology, Witten/Herdecke University, Children's Hospital Datteln, Datteln, Germany

⁷ Department of Neurology, Medical University of Vienna, Vienna, Austria

⁸ Division of Neuropathology and Neurochemistry, Department of Neurology, Medical University of Vienna, Vienna, Austria

Corresponding author

SUPPLEMENTARY METHODS

Flow cytometry assay for quantification of the TCC

Formation of the TCC was quantified by flow cytometry. Therefore, HEK293A cells were transfected with either MOG α_1 -EGFP or AQP4-M23-EmGFP as described in the methods part. Cells were harvested and resuspended in X-VIVO 15 media (Lonza) at a density of one million cells/ml. The cell suspensions were aliquoted at 100 μ l in a polypropylene 96-well microplate (Greiner, Kremsmünster, Austria), centrifuged at 300 g for 3 min and subsequently incubated with 10% heat-inactivated MOG-IgG or AQP4-IgG positive human serum samples together with 40% active or heat-inactivated human complement in X-VIVO 15 for 30 min at 37°C while shaking. Cells were washed three times with 10% heat-inactivated FCS (Sigma) in PBS (Sigma) containing 1 mM ethylenediamine tetraacetic acid (EDTA; Carl Roth, Karlsruhe, Germany) and blocked for 10 min using goat-IgG (Sigma; 20 μ g/ml) in FCS/PBS-EDTA buffer. Next, cells were incubated with mouse anti-C9neo antibody (clone WU13-15, Hycult Biotech; 5 μ g/ml) for 1 h at 4°C while shaking. After washing three times F(ab')₂-goat anti-mouse IgG (H+L) APC (eBioscience™, Thermo Fisher Scientific; 1 μ g/ml) was applied for 30 min at room-temperature while shaking. Subsequently, cells were washed three times in PBS-1 mM EDTA, resuspended in PBS-EDTA buffer containing 1:10 BD CellFIX™ (BD, Franklin Lakes, New Jersey, United States) for 10 min and transferred to polypropylene tubes (Corning, Corning, New York, United States). Analysis was done using an Accuri™ C6 Flow Cytometer (BD) together with the BD Accuri™ C6 Software (version 1.0.264.21, BD), where HEK293A cells were gated using forward and side scatter (at a minimum of 10000 events), single cells were separated and the TCC signal was quantified in the FL-4 channel (APC) of EGFP or EmGFP (FL-1) positive cells. The FL-4 mean fluorescence intensity (MFI) is given as difference between cells incubated with active and heat-inactivated human complement.

Immunocytochemistry of TCC and C3

Deposition of TCC and C3 on the cell surfaces were determined through staining of HEK293A cells transfected with MOG and AQP4 constructs or empty vectors (see methods part), that were incubated with either 10% MOG-IgG or AQP4-IgG positive human serum samples or control serum (heat-inactivated) or rh8-18-C5 or E5415A (both at 5 μ g/ml) together with 40% active or heat-inactivated human complement in X-VIVO 15 buffer for 45 min at 37°C. Subsequently, cells were washed three times with 10% heat-inactivated FCS in PBS and blocked for 10 min with goat-IgG (20 μ g/ml) in FCS/PBS buffer. Next, cells were incubated with either mouse anti-C9neo antibody (5 μ g/ml) or mouse anti-C3 antibody (clone 10C7, Cedarlane; at 7.5 μ g/ml) in FCS/PBS buffer for 1 h at 4°C while shaking. After washing again, cells were stained with goat anti-mouse IgG1 Alexa Fluor™ 594 antibody (Invitrogen, Carlsbad, California, United States; at 1:1000 in FCS/PBS buffer) for 30 min at room

temperature. Cells were washed again and 4',6-diamidino-2-phenylindole (DAPI; Sigma; 1:10000 in PBS) was added to the cells to stain the nuclei.

Staining was evaluated on either the Operetta® CLS™ High Content Analysis System (PerkinElmer, Waltham, Massachusetts, United States; eFigures 7, 8, 9, 10, 11, 12) or a Leica DMI8 (Leica Microsystems, Wetzlar, Germany; eFigure 13). For picture acquisition with the Operetta® EGFP/EmGFP was excited at 475 nm, DAPI at 365 nm and Alexa Fluor™ 594 at 550 nm and z-stacks of the pictures were taken. Furthermore, deconvolution was executed using the Huygens Professional Software (version 21.10; Scientific Volume Imaging, Hilversum, The Netherlands; Classic Maximum Likelihood Estimation). Fiji ImageJ (version 2.0) was used for generating maximum projections of the z stacks and further picture processing, including brightness and contrast adjustments.

Flow cytometry analysis of complement inhibitors CD46 and CD59

For the analysis of complement inhibitors CD46 and CD59 HEK293A cells, either untreated or transfected with pEGFP-N1-MOG α_1 -STOP (see methods part) or AQP4-M23-STOP (Vivid Colours™ pcDNA™ 6.2-EmGFP plasmid without EmGFP tag), were harvested after 24 h, 24 h or 48 h, respectively. Two FACS tubes (Falcon®, Corning) per cell line (containing one million cells) were prepared and cells were washed with a buffer containing 0.5% BSA (Carl Roth) and 0.1% sodium azide (Carl Roth) in D-PBS (Sigma) and incubated with either 50 μ l buffer alone (as gating control) or with 50 μ l of a mixture containing 5 μ l of the following antibodies: mouse anti-human CD59 APC (clone MEM-43, ImmunoTools, Friesoythe, Germany), mouse anti-human/bovine CD46 FITC (clone MEM-258, ImmunoTools) and mouse anti-human HLA-A, B, C PE/Cyanine7 (clone W6/32, BioLegend, San Diego, California, United States; as a staining control) for 30 min at 4°C. After washing again, cells were resuspended in buffer additionally containing 1% L-Glutamine (Sigma) and 4% PFA (Carl Roth) and measured using a BD FACSVerse™ (BD) according to the manufacturer's instructions. Cells were gated using forward and side scatter (at a minimum of 10000 events) and single cells were separated. Data were analyzed using Flowing Software (version 2.5.1, Turku Centre for Biotechnology, University of Turku, Finland) and are given as % of positive cells per population.

Flow cytometry analysis of transfection efficiencies

Transfection efficiencies of HEK293A cells transfected with either AQP4-M23-EmGFP or different MOG isoforms (MOG $\alpha_{1-3}\beta_{1-3}$ -EGFP, see methods section) were analyzed by flow cytometry. Therefore, transfected cells were harvested after 24 h or 48 h, for MOG and AQP4, respectively, and transferred to a 96-well polypropylene plate at a density of 1 million cells per ml in a buffer containing 1 mM EDTA in PBS. Cells were fixed using 1:10 BD CellFIX™ in PBS-EDTA for 10 min. Subsequently, cells were washed with 10% heat-inactivated FCS in PBS-

EDTA and 5 µg/ml mouse 8-18-C5 (for MOG staining¹), 5 µg/ml E5415A (for AQP4 staining, see methods part) or 5 µg/ml mouse-IgG as negative control (MCA928, Bio-Rad, Hercules, California, United States) was added. After 1 h incubation at 4°C while shaking cells were washed again and incubated with F(ab')₂-goat anti-mouse IgG (H+L) APC (1 µg/ml) for 30 min at room-temperature while shaking. Cells were washed with PBS-EDTA, resuspended in PBS-EDTA buffer containing 1:10 BD CellFIX™ for 10 min and transferred to polypropylene tubes. Analysis was done with an Accuri™ C6 Flow Cytometer together with the BD Accuri™ C6 Software, where HEK293A cells were gated using forward and side scatter (at a minimum of 10000 events), single cells were separated and the APC and EGFP/EmGFP signals were analyzed in the FL-4 and FL-1 channel, respectively.

SUPPLEMENTARY RESULTS

eTable 1: Demographic, clinical and immunological characteristics of the subgroup of 42 included patients without clinical information on disease course and acute relapse at sampling

	MOG-IgG positive (n=29) ^a	AQP4-IgG positive (n=13) ^b	Difference MOGAD-NMOSD
MOG-IgG titer (1:), median with range	1280 (640-10240)		
MOG-IgG binding pattern			
isoform $\alpha_1\beta_1$	5 (17%)		
isoform $\alpha_{1-3}\beta_1$	10 (35%)		
isoform $\alpha_{1-3}\beta_{1-3}$	14 (48%)		
AQP4-IgG titer (1:), median with range		1280 (160-10240)	
Complement-dependent cytotoxicity ^c	7.9 (2.2-24.4)	29.0 (4.6-44.7)	-21.1 (-28.8 to -10.9) ^e
Sex			
Females	15 (52%)	11 (85%)	0.19 (0.04 to 1.04) ^f
Males	14 (48%)	2 (15%)	
Age (years, median with range) ^d	37 (3-76)	53 (26-98)	-18.7 (-32.9 to -0.8) ^e
Age groups ^d			
Children (<18 years)	10 (34%)	0 (0%)	14.5 (0.78 to 269.7) ^f
Adults (≥ 18 years)	19 (66%)	13 (100%)	

^a demyelinating phenotype consistent with MOG-IgG associated disorders (MOGAD), ^b neuromyelitis optica spectrum disorders (NMOSD), ^c median % lysis with range, ^d at the time sample was taken, ^e Woolf's logit odds ratio with 95% confidence interval, ^f Hodges-Lehman median difference with 95% confidence interval

eTable 2: Demographic, clinical and immunological characteristics of the subgroup of 65 included patients with clinical information on disease course but without information on acute relapse at sampling

	MOG-IgG positive (n=39) ^a	AQP4-IgG positive (n=26) ^b	Difference MOGAD-NMOSD
MOG-IgG titer (1:), median with range	1280 (160-10240)		
MOG-IgG binding pattern			
isoform $\alpha_1\beta_1$	12 (31%)		
isoform $\alpha_{1-3}\beta_1$	10 (25%)		
isoform $\alpha_{1-3}\beta_{1-3}$	17 (44%)		
AQP4-IgG titer (1:), median with range		1280 (20-163840)	
Complement-dependent cytotoxicity ^c	6.4 (1.9-37.6)	25.6 (3.7-44.3)	-13.9 (-22.1 to -5.8) ^e
Sex			
Females	20 (51%)	25 (96%)	0.04 (0.01 to 0.24) ^f
Males	19 (49%)	1 (4%)	
Age (years, median with range) ^d	16 (0-74)	47 (3-84)	-22.7 (-34.1 to -7.4) ^e
Age groups ^d			
Children (<18 years)	22 (56%)	5 (19%)	5.44 (1.70 to 17.38) ^f
Adults (≥ 18 years)	17 (44%)	21 (81%)	
Disease course ^d			
Relapsing	25 (64%)	18 (69%)	0.79 (0.28 to 2.29) ^f
Monophasic	14 (36%)	8 (31%)	

^a demyelinating phenotype consistent with MOG-IgG associated disorders (MOGAD), ^b neuromyelitis optica spectrum disorders (NMOSD), ^c median % lysis with range, ^d at the time sample was taken, ^e Woolf's logit odds ratio with 95% confidence interval, ^f Hodges-Lehman median difference with 95% confidence interval.

eTable 3: Demographic, clinical and immunological characteristics of the subgroup of 42 included patients with clinical information on disease course and acute relapse at sampling

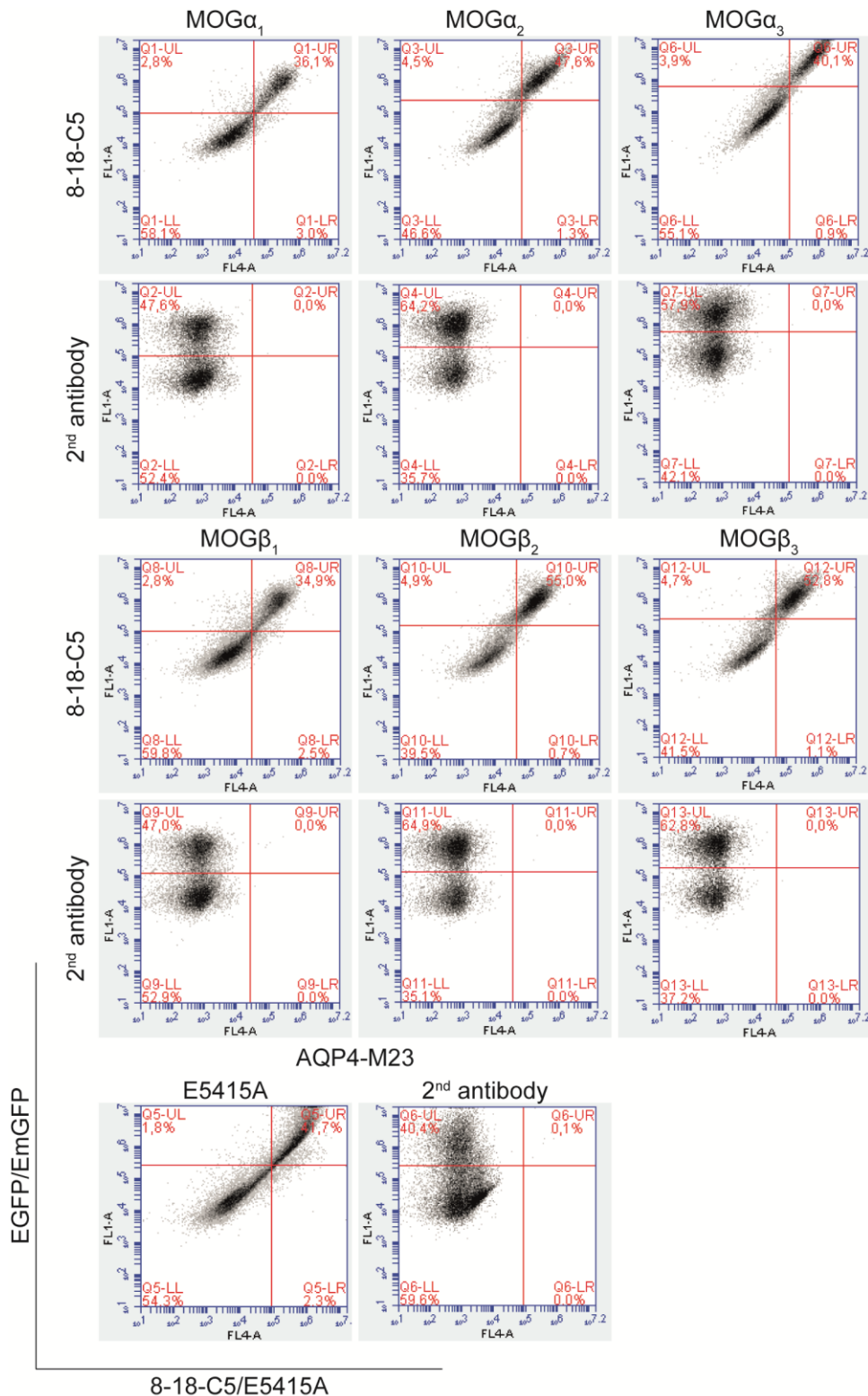
	MOG-IgG positive (n=30) ^a	AQP4-IgG positive (n=12) ^b	Difference MOGAD-NMOSD
MOG-IgG titer (1:), median with range	1280 (160-5120)		
MOG-IgG binding pattern			
isoform $\alpha_1\beta_1$	8 (27%)		
isoform $\alpha_{1-3}\beta_1$	9 (30%)		
isoform $\alpha_{1-3}\beta_{1-3}$	13 (43%)		
AQP4-IgG titer (1:), median with range		2560 (20-163840)	
Complement-dependent cytotoxicity ^c	6.0 (1.9-14.1)	27.7 (5.1-44.3)	-21.7 (-26.4 to -8.1) ^e
Sex			
Females	17 (57%)	11 (92%)	0.12 (0.01 to 1.04) ^f
Males	13 (43%)	1 (8%)	
Age (years, median with range) ^d	12 (0-74)	50 (7-79)	-27.5 (-40.9 to -2.2) ^e
Age groups ^d			
Children (<18 years)	20 (67%)	4 (33%)	4.00 (0.97 to 16.55) ^f
Adults (≥ 18 years)	10 (33%)	8 (67%)	
Disease course ^d			
Relapsing	19 (63%)	8 (67%)	0.86 (0.21 to 3.54) ^f
Monophasic	11 (37%)	4 (33%)	
Acute relapse at sampling ^d			
Relapse	9 (30%)	6 (50%)	0.36 (0.08 to 1.48) ^f
Remission	21 (70%)	6 (50%)	

^a demyelinating phenotype consistent with MOG-IgG associated disorders (MOGAD), ^b neuromyelitis optica spectrum disorders (NMOSD), ^c median % lysis with range, ^d at the time sample was taken, ^e Woolf's logit odds ratio with 95% confidence interval, ^f Hodges-Lehman median difference with 95% confidence interval.

eTable 4: Influence of disease course and acute relapses on complement-dependent cytotoxicity and antibody titers

Clinical information on disease course (n=65)^a	MOG-IgG positive (n=39)^b	AQP4-IgG positive (n=26)^c
Complement-dependent cytotoxicity ^d		
Relapsing	6.25 (1.86-37.64)	26.56 (6.18-44.29)
Monophasic	6.78 (2.37-26.67)	16.21 (3.66-33.26)
Median difference ^e	-0.87 (-2.92 to 0.81)	5.69 (-5.03 to 19.95)
Antibody titer (1:), median with range		
Relapsing	1280 (160-10240)	2560 (20-163840)
Monophasic	1280 (160-10240)	480 (20-20480)
Median difference ^e	-640 (-1000 to 0)	1920 (-120 to 19840)
Clinical information on disease course and acute relapse (n=42)^a	MOG-IgG positive (n=30)^b	AQP4-IgG positive (n=12)^c
Complement-dependent cytotoxicity ^d		
Relapse	5.43 (2.37-13.80)	28.94 (6.91-44.29)
Remission	5.99 (1.86-14.13)	19.82 (5.08-37.70)
Median difference ^e	-0.29 (-2.32 to 1.53)	10.31 (-6.18 to 29.47)
Antibody titer (1:), median with range		
Relapsing	1280 (160-2560)	61440 (160-163840)
Monophasic	1280 (320-5120)	720 (20-20480)
Median difference ^e	0 (-640 to 0)	51190 (-640 to 143360)

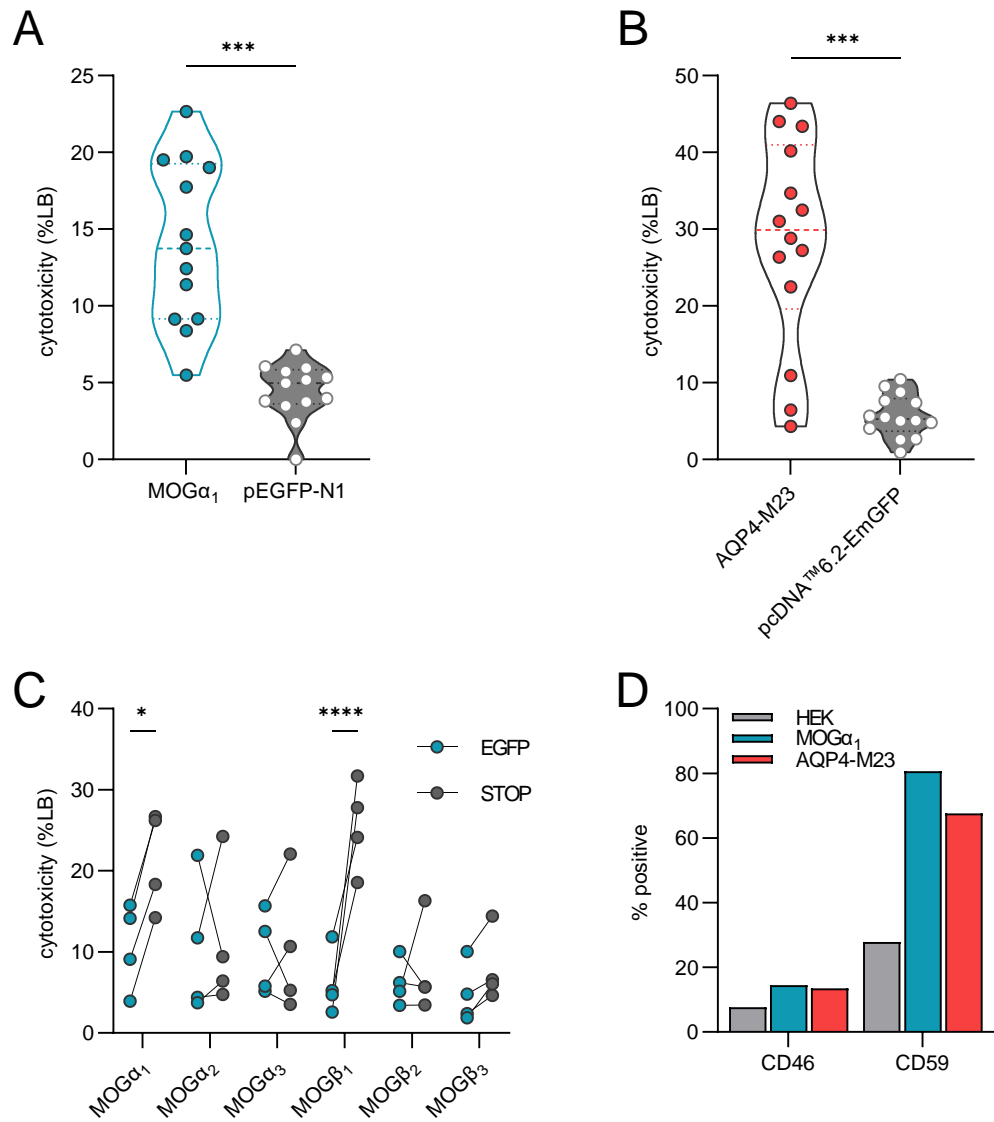
^a at the time sample was taken, ^b demyelinating phenotype consistent with MOG-IgG associated disorders (MOGAD), ^c neuromyelitis optica spectrum disorders (NMOSD), ^d median % lysis with range, ^e Hodges-Lehman median difference with 95% confidence interval.



eFigure1: Transfection efficiencies of the MOG isoforms and AQP4-M23

Expression of different MOG isoforms (MOG α_{1-3} -EGFP, upper panels) or AQP4-M23-EmGFP (lower panel) was analyzed using flow cytometry after staining with the monoclonal mouse anti-MOG 8-18-C5 or the mouse anti-AQP4 E5415A antibody. Antibody staining was visualized in the FL-4 channel using an APC conjugated anti-mouse 2nd antibody. Shown are

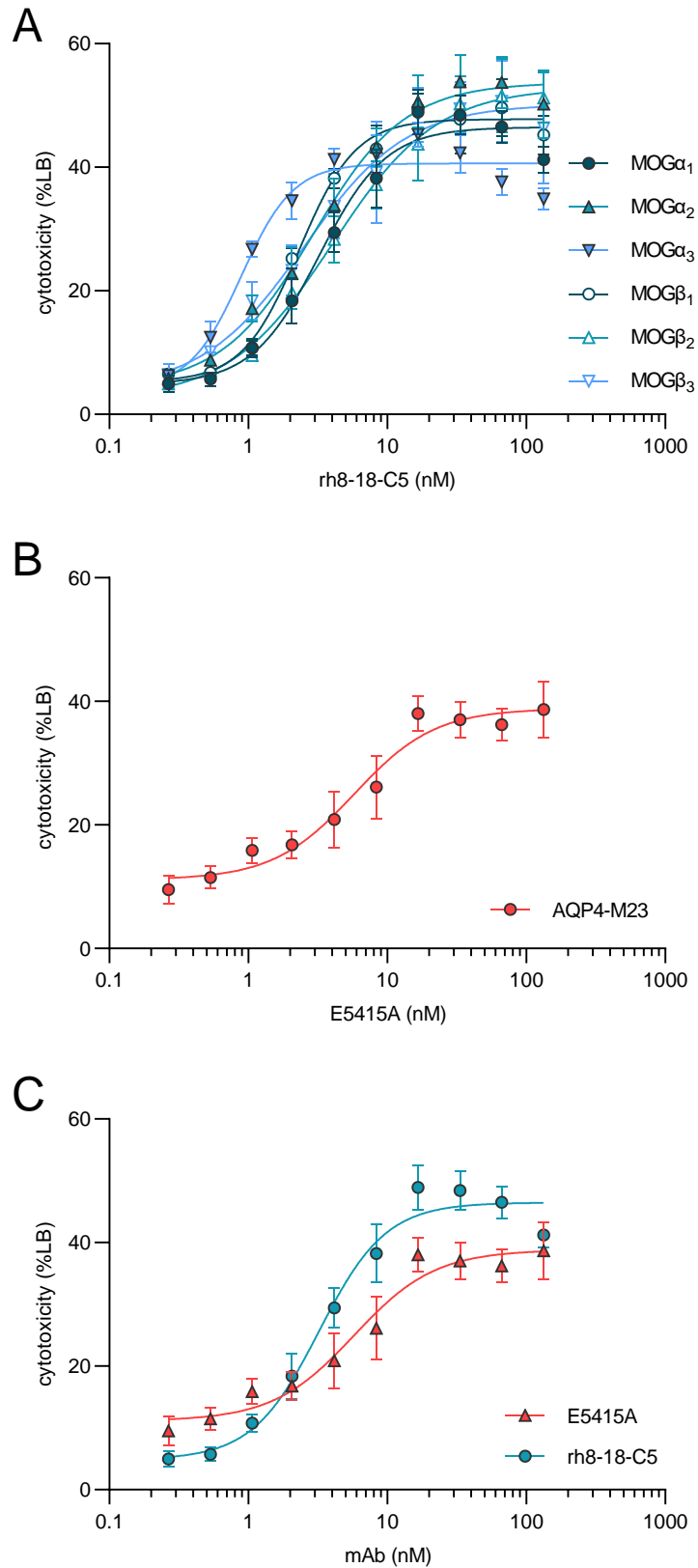
scatter plots of the FL-1 (EGFP or EmGFP) and FL-4 (anti-mouse APC) channels of cells stained with rh8-18-C5 or E5415A together with 2nd antibody or 2nd antibody only as control.



eFigure 2: Specificity of the LDH assay and influence of the EGFP tag and complement inhibitors

CDC (as percentage of lysis buffer; violin plots: dashed line: median, dotted lines: quartiles) is shown A: for 13 human serum samples positive for MOG-IgG on HEK293A cells expressing MOG α_1 -EGFP (blue) or pEGFP-N1 (empty expression vector; grey) and B: AQP4-M23-EmGFP (red) or pcDNA™6.2-EmGFP (empty expression vector; grey) expressing cells after treatment of AQP4-IgG positive serum samples (n=14) with human complement. Wilcoxon matched-pairs signed rank test: *** p<0.001. C: Comparison of complement activation (as percentage of lysis buffer) of four human MOG-IgG positive sera on either MOG-EGFP (blue) or without EGFP tag (STOP; grey) on six different MOG isoforms (MOG α_{1-3} , MOG β_{1-3}). Two-way ANOVA with post-hoc Šídák's test: * p=0.0253, **** p<0.0001. D: Flow cytometry analysis of the expression of two complement inhibitors CD46 and CD59 on the surface of HEK293A cells (grey) and HEK cells transfected with either MOG α_1 (blue) or AQP4-M23 (red). Shown is

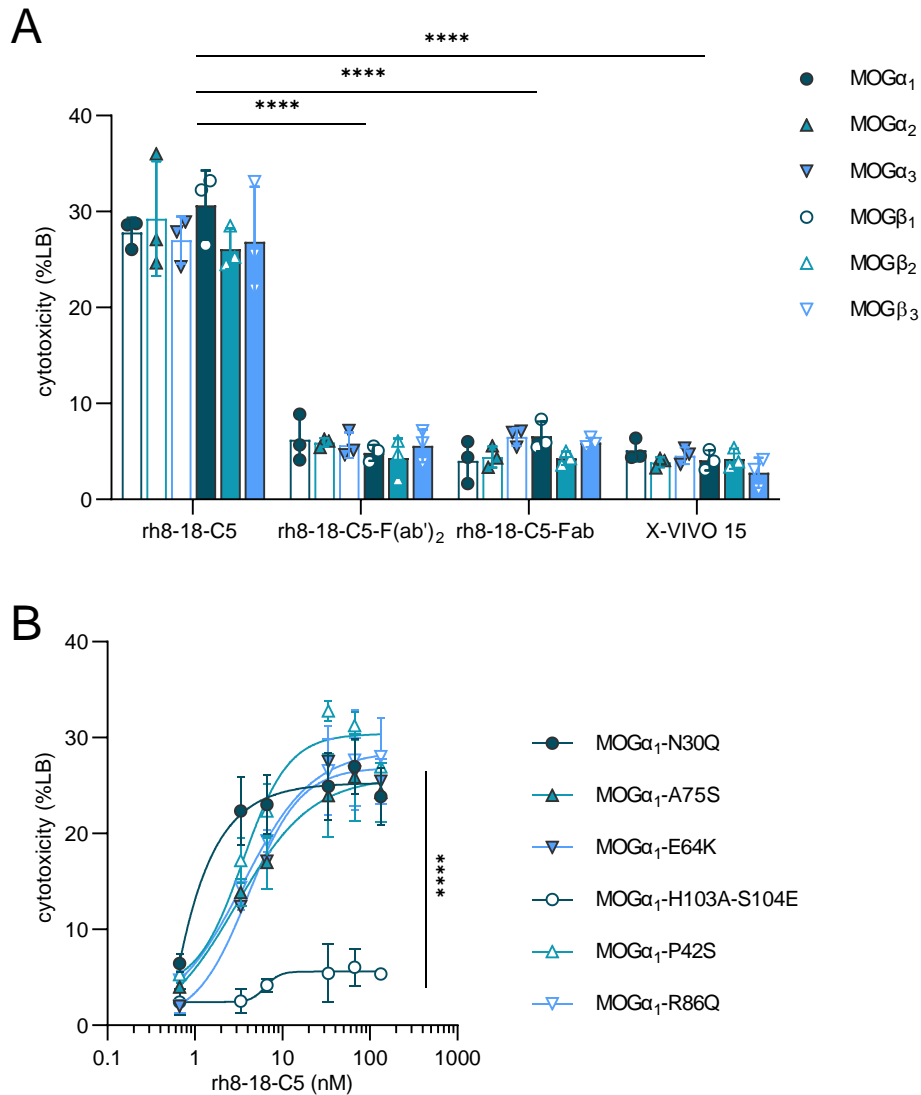
the percentage of positive stained cells. AQP4=aquaporin 4, CDC=complement-dependent cytotoxicity, LB=lysis buffer, MOG=myelin oligodendrocyte glycoprotein



eFigure 3: Complement activation of rh8-18-C5 and E5415A mAbs

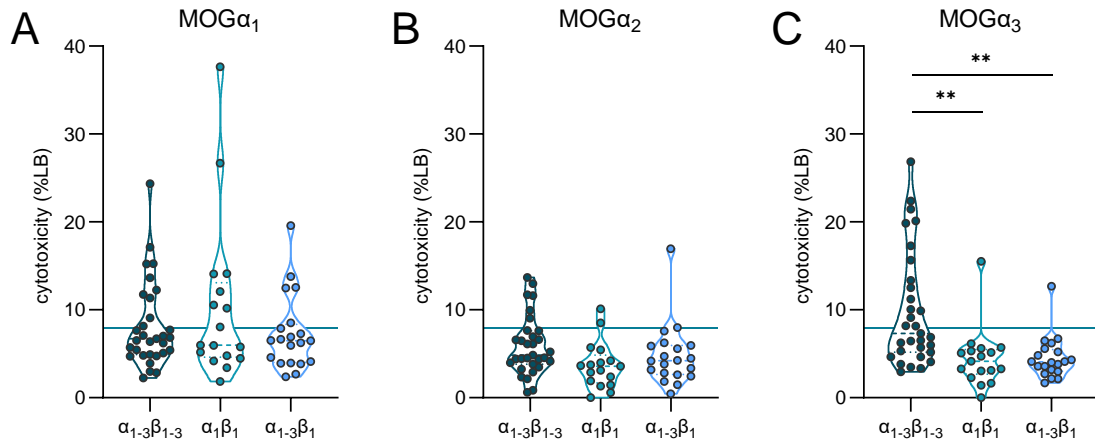
Shown is the CDC (as percentage to lysis buffer) plotted against the concentration of A: rh8-18-C5 on six different MOG isoforms (MOG α_{1-3} , MOG β_{1-3}), or B: E5415A on AQP4-M23

transfected cells, or C: rh-8-18C5 on MOG α_1 and E5415A on AQP4-M23. Shown is the mean with SEM of three experiments. Curves were fitted to a non-linear four parameter equation and EC₅₀ (95% CI) values are as follows: MOG α_1 : 3.2 (2.2-4.3), MOG α_2 : 2.9 (1.6-4.3), MOG α_3 : 0.9 (0.6-1.2), MOG β_1 : 2.3 (1.7-2.9), MOG β_2 : 4.1 (2.1-6.1), MOG β_3 : 2.5 (0.3-4.7), AQP4-M23: 5.8 (2.3-9.2); the maximum lysis values are (in % to lysis buffer, 95% CI): MOG α_1 : 46.5 (42.8-50.1), MOG α_2 : 53.7 (48.5-58.9), MOG α_3 : 40.6 (38.2-43.0), MOG β_1 : 47.8 (44.8-50.7), MOG β_2 : 52.9 (46.3-59.5), MOG β_3 : 50.2 (42.3-58.1), AQP4-M23: 38.8 (33.6-44.1). AQP4=aquaporin 4, CDC=complement-dependent cytotoxicity, LB=lysis buffer, mAb=monoclonal antibody, MOG=myelin oligodendrocyte glycoprotein



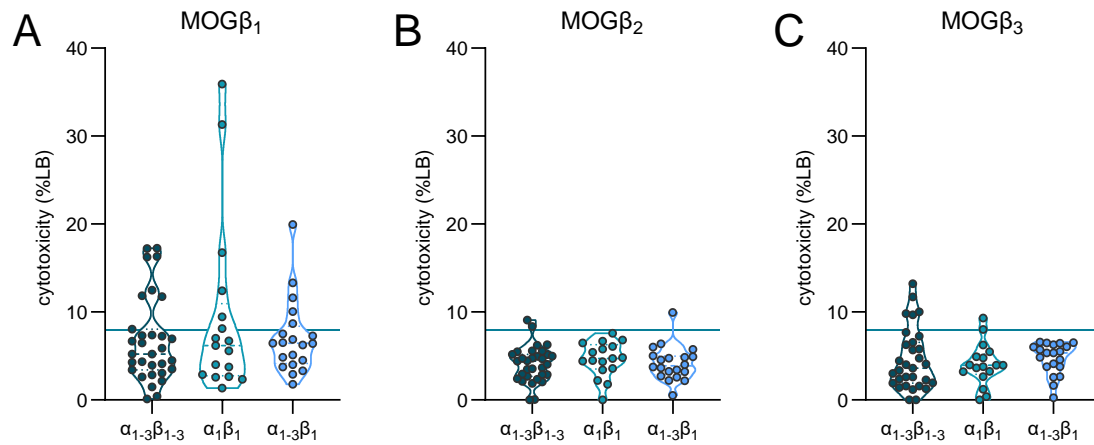
eFigure 4: CDC of rh8-18-C5 Fab and F(ab')₂ fragments and on MOGα₁ sequence variants

A: Shows CDC of rh8-18-C5 and Fab and F(ab')₂ fragments of rh8-18-C5 (at 10 µg/ml) or X-VIVO 15 buffer on six different MOG isoforms (MOGα₁₋₃, MOGβ₁₋₃) as percentage of lysis buffer. The bars indicate the mean with SD of three experiments. Asterisks show a significant difference between groups for all MOG isoforms tested. Two-way ANOVA with post-hoc Tukey's: **** p<0.0001. B: CDC (as percentage to lysis buffer) is plotted against the concentration of rh8-18-C5 on different MOGα₁ variants. Curves were fitted to a non-linear four parameter equation. Shown is the mean with SEM of three experiments. Asterisks indicate statistical difference at the highest concentration (133 nM) for all variants compared to the H103A/S104E mutation. Two-way ANOVA with post-hoc Tukey's: **** p<0.0001. CDC=complement-dependent cytotoxicity, LB=lysis buffer, MOG=myelin oligodendrocyte glycoprotein



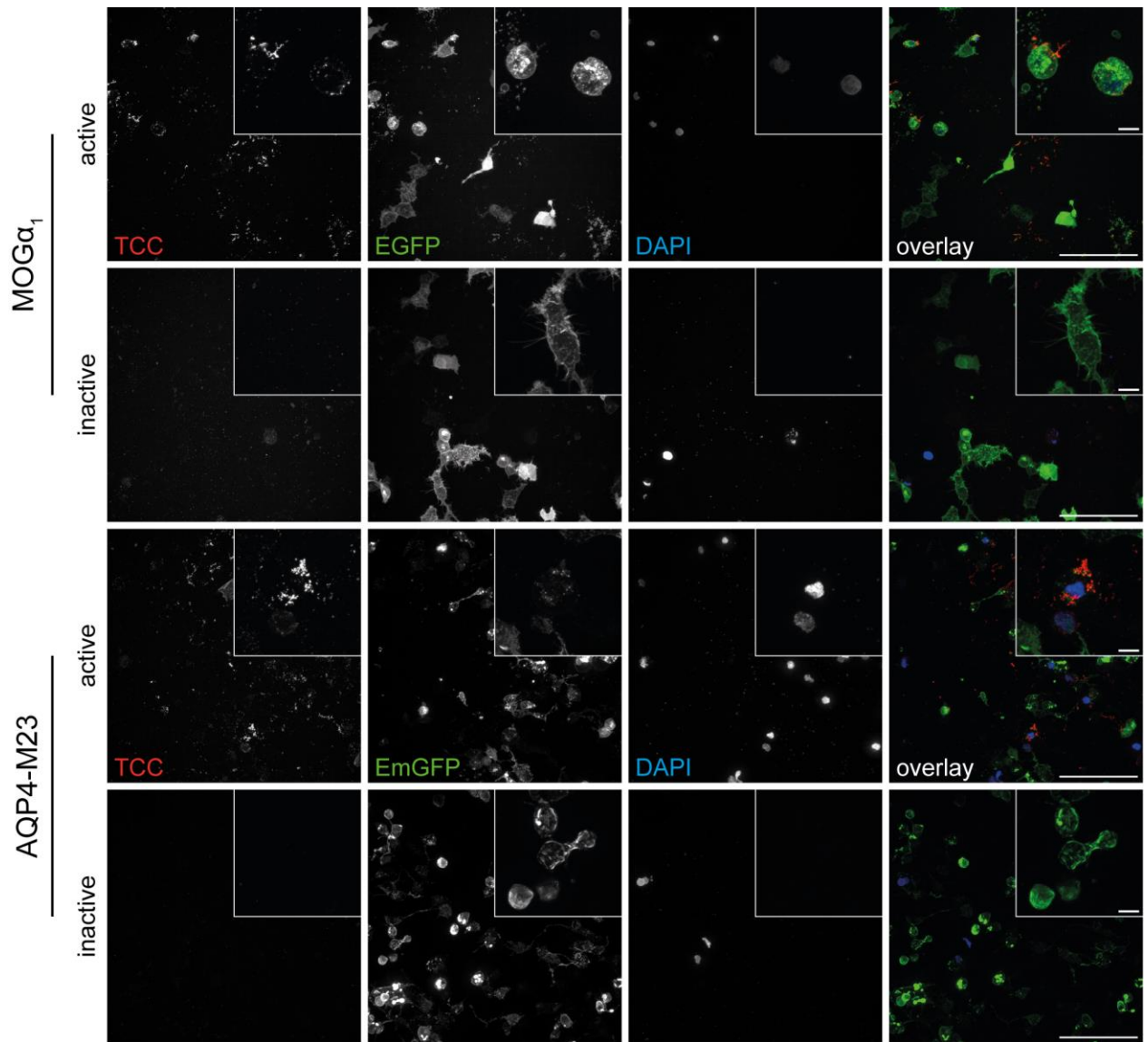
eFigure 5: Complement activation of distinct human MOG-IgG binding patterns on MOG α_{1-3}

Violin plots (dashed line: median, dotted lines: quartiles) show the CDC (as percentage to lysis buffer) of human MOG-IgG positive serum samples on A: MOG α_1 , B: MOG α_2 and C: MOG α_3 according to the binding pattern (' $\alpha_{1-3}\beta_{1-3}$ ', n=31; ' $\alpha_1\beta_1$ ', n=17; ' $\alpha_{1-3}\beta_1$ ', n=20) of the samples, as indicated. The solid line indicates the cut-off value (mean+2*SD of cells treated with complement only). Kruskal-Wallis test with post-hoc Dunn's: ** p<0.01. CDC=complement-dependent cytotoxicity, LB=lysis buffer, MOG=myelin oligodendrocyte glycoprotein



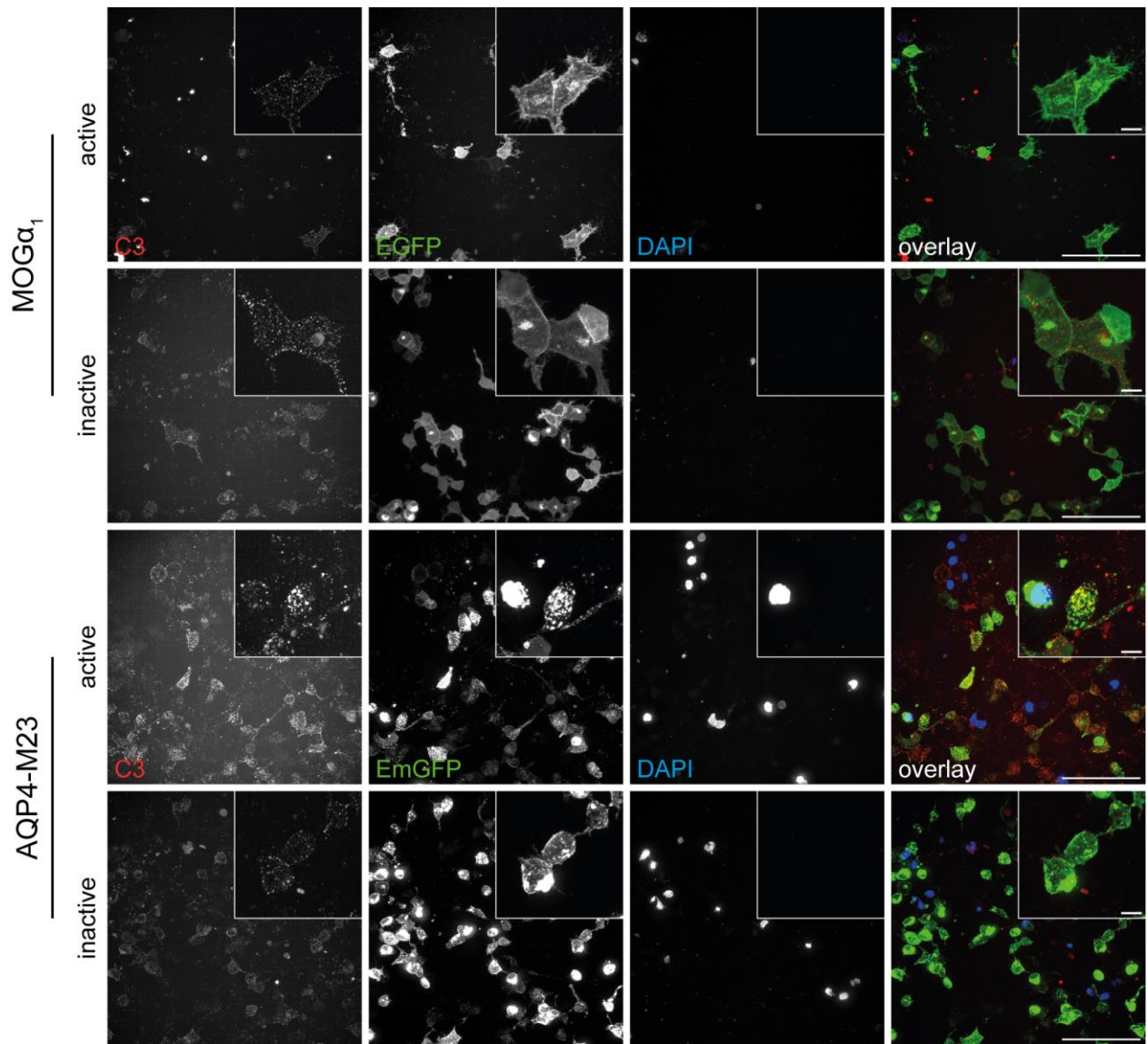
eFigure 6: Complement activation of distinct human MOG-IgG binding patterns on MOGβ₁₋₃

CDC (as percentage to lysis buffer; violin plots: dashed line: median, dotted lines: quartiles) of human MOG-IgG positive serum samples on A: MOGβ₁, B: MOGβ₂ and C: MOGβ₃ is demonstrated on violin plots according to their binding pattern (‘α₁₋₃β₁₋₃’, n=31; ‘α₁β₁’, n=17; ‘α₁₋₃β₁’, n=20). The solid line indicates the cut-off value (mean+2*SD of cells treated with complement only). CDC=complement-dependent cytotoxicity, LB=lysis buffer, MOG=myelin oligodendrocyte glycoprotein



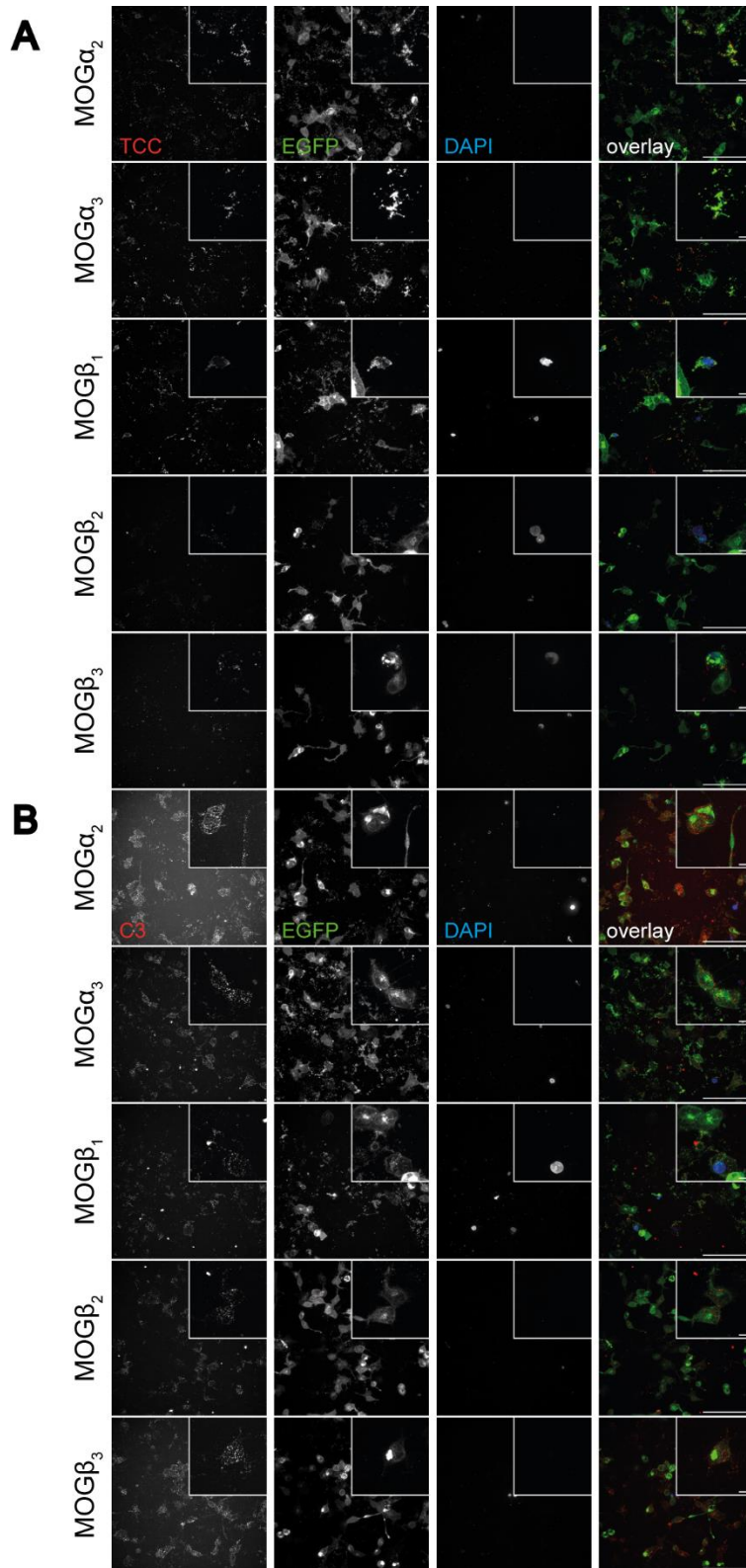
eFigure 7: TCC deposition on MOG and AQP4 expressing cells

Immunocytochemistry showing TCC deposition on MOG α_1 -EGFP (upper two panels) or AQP4-M23-EmGFP (lower two panels) after treatment with representative human serum samples positive for MOG-IgG or AQP4-IgG, respectively, together with active or heat-inactivated human complement, as indicated. Pictures are shown in grayscale and as composite (TCC: red, EGFP/EmGFP: green, DAPI: blue) and insets show a magnified area of the respective images. Scale bar=100 μ m, Inset scale bar=10 μ m. AQP4=aquaporin 4, MOG=myelin oligodendrocyte glycoprotein, TCC=terminal complement complex.



eFigure 8: Staining of C3/C3b/iC3b on MOG and AQP4 expressing cells after complement activation

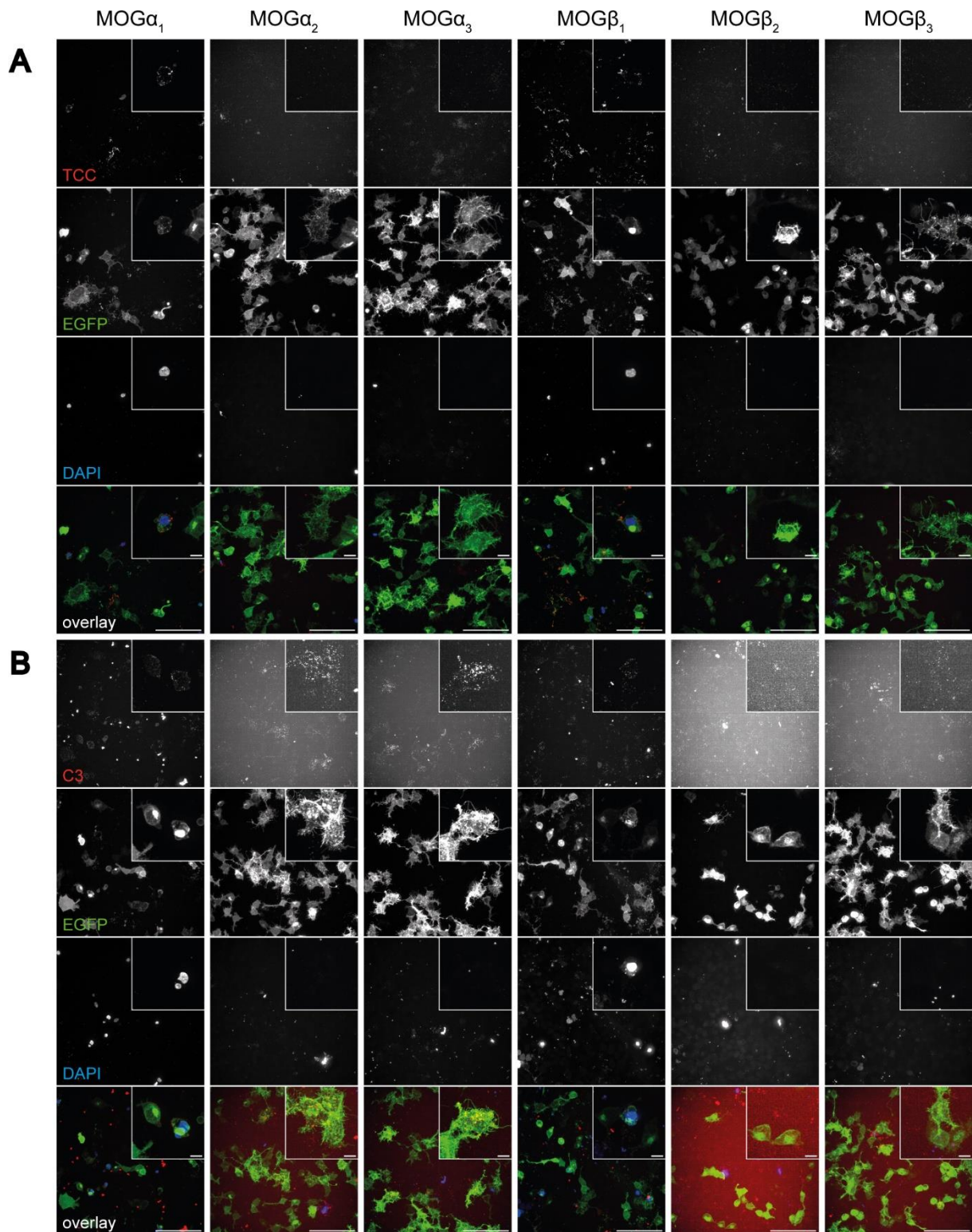
C3/C3b/iC3b deposition on HEK293A cells expressing MOG α_1 -EGFP (upper panels) or AQP4-M23-EmGFP (lower panels) after incubation with human serum samples positive for MOG-IgG or AQP4-IgG, respectively, together with active or inactivated human complement is pictured. Grayscale images and composites are shown (C3/C3b/iC3b: red, EGFP/EmGFP: green, DAPI: blue). Insets show a magnified area of the respective images. Scale bar=100 μ m, Inset scale bar=10 μ m. AQP4=aquaporin 4, C3=complement component 3, MOG=myelin oligodendrocyte glycoprotein.



eFigure 9: TCC and C3/ C3b/iC3b staining on MOG α_{2-3} and MOG β_{1-3} after complement activation by a human ' $\alpha_{1-3}\beta_{1-3}$ ' pattern MOG-IgG positive serum sample

Cell surface deposition of A: TCC and B: C3/C3b/iC3b is shown on HEK293A cells expressing MOG α_{2-3} and MOG β_{1-3} fused to EGFP after incubation with an ' $\alpha_{1-3}\beta_{1-3}$ ' pattern human MOG-IgG serum sample in combination with active complement. Grayscale images of TCC or C3/C3b/iC3b (red), EGFP (green), DAPI (blue) and composite pictures are shown. Insets show

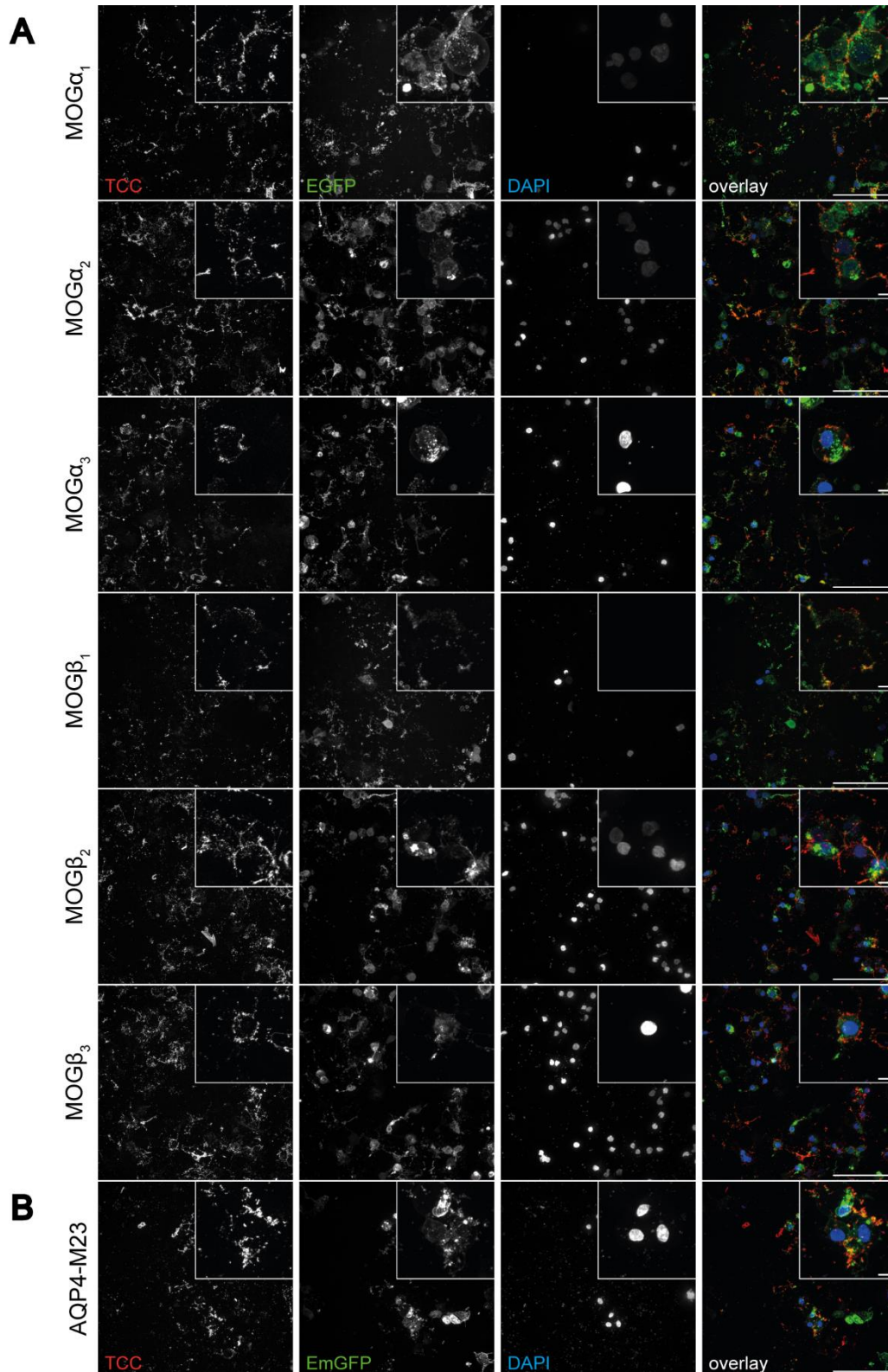
a magnified area of the respective images. Scale bar=100 μm , Inset scale bar=10 μm .
C3=complement component 3, MOG=myelin oligodendrocyte glycoprotein, TCC=terminal complement complex



eFigure 10: TCC and C3/C3b/iC3b staining on MOG α_{1-3} and MOG β_{1-3} after complement activation by a human ' $\alpha_1\beta_1$ ' pattern MOG-IgG positive serum sample

A: TCC and B: C3/C3b/iC3b stainings are shown for six MOG isoforms (MOG α_{1-3} , MOG β_{1-3}) fused to EGFP after complement activation by a human MOG-IgG serum sample belonging to the ' $\alpha_1\beta_1$ ' binding pattern. Images are shown as grayscale (TCC or C3/C3b/iC3b (red), EGFP (green), DAPI (blue)) or composites. Insets show a magnified area of the respective images.

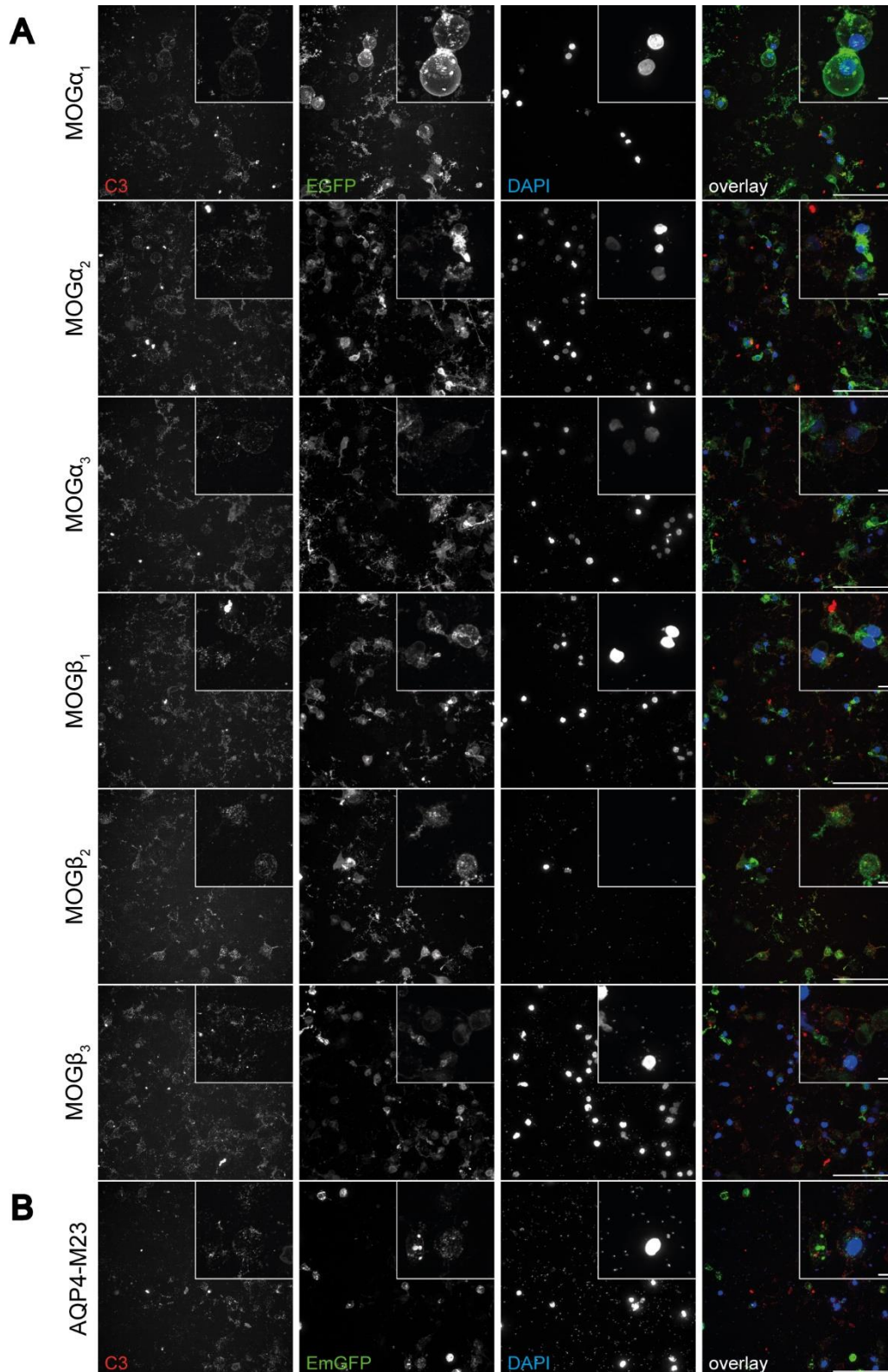
Scale bar=100 μm , Inset scale bar=10 μm . C3=complement component 3, MOG=myelin oligodendrocyte glycoprotein, TCC=terminal complement complex



eFigure 11: TCC staining of rh8-18-C5 and E5415A induced complement activation

Deposition of TCC on HEK293A cells expressing A: different MOG isoforms (MOG α_{1-3} , MOG β_{1-3}) fused to EGFP induced by complement activation by rh8-18-C5 or B: AQP4-M23-EmGFP after complement activation by E5415A is shown. Images are shown as grayscale (TCC (red), EGFP/EmGFP (green), DAPI (blue)) or composites. Insets show a magnified area of the

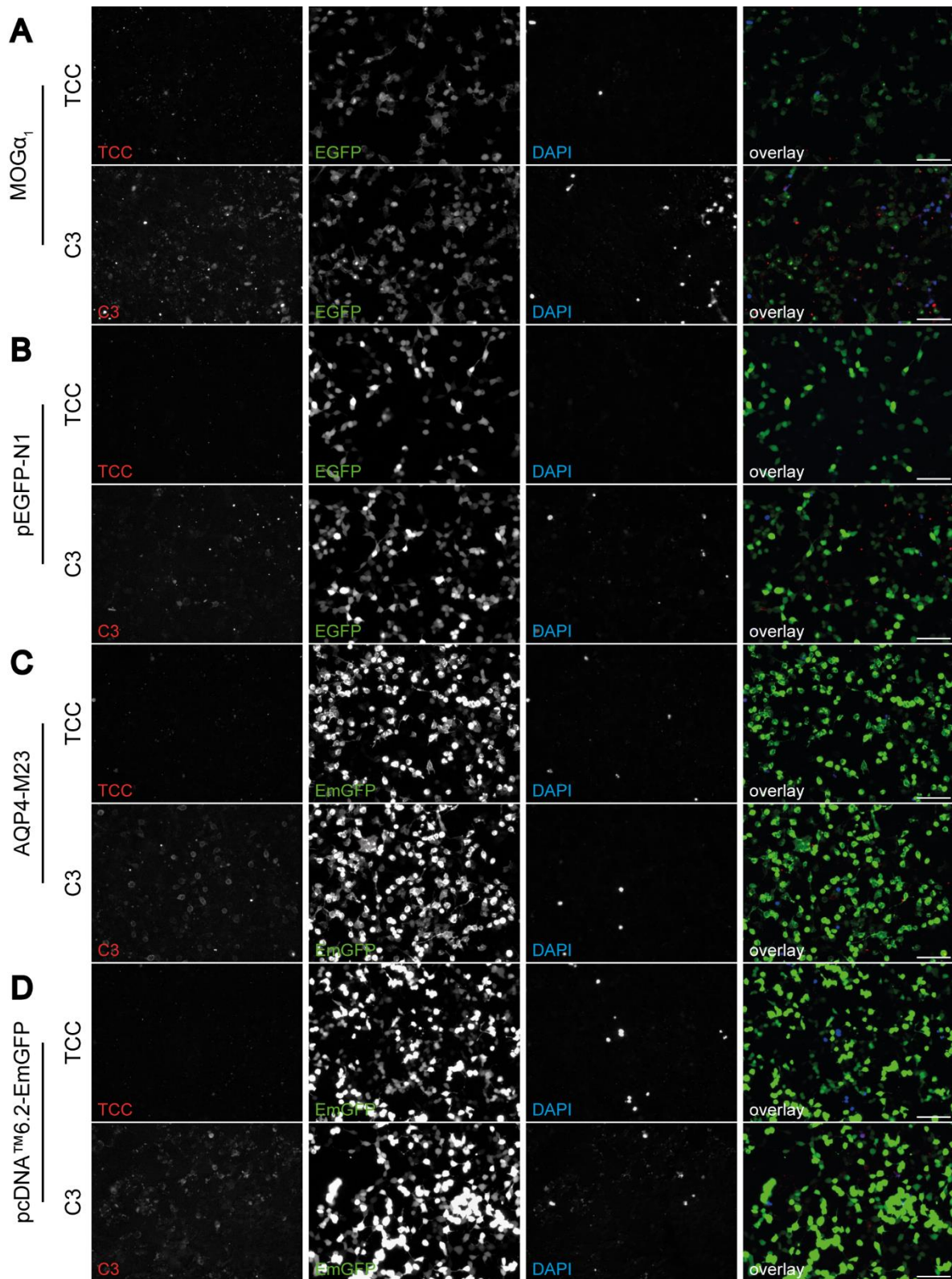
respective images. Scale bar=100 μm , Inset scale bar=10 μm . AQP4=aquaporin 4, MOG=myelin oligodendrocyte glycoprotein, TCC=terminal complement complex



eFigure 12: C3/C3b/iC3b staining of rh8-18-C5 and E5415A induced complement activation

Cell surface deposition of complement proteins C3/C3b/iC3b is shown on HEK293A cells expressing A: different MOG isoforms (MOG α_{1-3} , MOG β_{1-3}) fused to EGFP after complement activation by rh8-18-C5 or B: AQP4-M23-EmGFP after complement activation by E5415A. Images are shown as grayscale (C3/C3b/iC3b (red), EGFP/EmGFP (green), DAPI (blue)) or

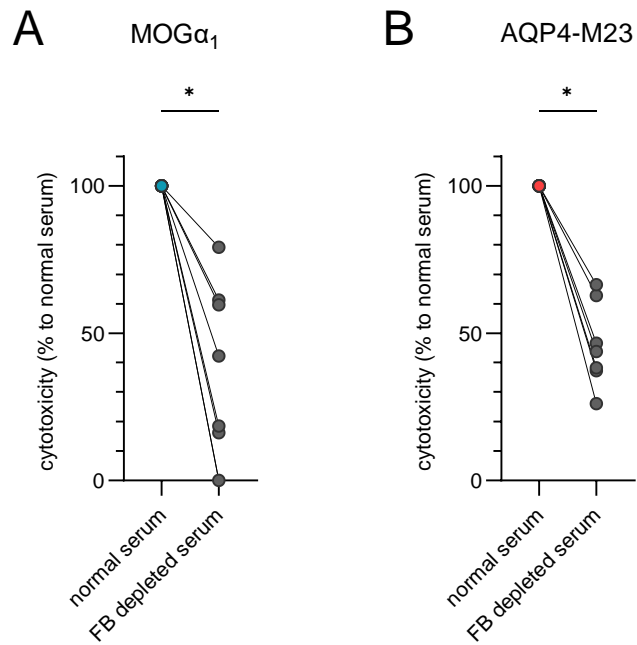
composites. Insets show a magnified area of the respective images. Scale bar=100 μm , Inset scale bar=10 μm . AQP4=aquaporin 4, C3: complement component 3, MOG=myelin oligodendrocyte glycoprotein



eFigure 13: TCC and C3/C3b/iC3b staining on transfection controls and with a MOG-IgG and AQP4-IgG double negative serum sample

A representative MOG-IgG and AQP4-IgG double negative serum sample was incubated on A: MOG α_1 -EGFP or B: AQP4-M23-EmGFP expressing HEK293A cells together with active human complement. C: Complement activation by a human MOG-IgG positive serum sample on pEGFP-N1 or D: a human AQP4-IgG positive serum sample on pcDNA™6.2-EmGFP

transfected HEK293A cells is computed. Grayscale images of TCC or C3/C3b/iC3b (red), EGFP/EmGFP (green), DAPI (blue) and composite pictures are shown. Insets show a magnified area of the respective images. Scale bar=100 μm , Inset scale bar=10 μm . AQP4=aquaporin 4, C3: complement component 3, MOG=myelin oligodendrocyte glycoprotein, TCC=terminal complement complex



eFigure 14: Reduced cytotoxicity after incubation with factor B depleted serum

LDH cytotoxicity assay of HEK293A cells expressing A: $\text{MOG}\alpha_1$ -EGFP or B: AQP4-M23-EmGFP after incubation with human serum samples harboring MOG-IgG (A; n=9) or AQP4-IgG (B; n=9) together with either normal human serum or factor B-depleted human serum as complement source. Data were normalized to the cytotoxicity after incubation with normal human serum. Wilcoxon test: MOG: * p=0.0117; AQP4: * p=0.0195. FB=factor B

SUPPLEMENTARY REFERENCES

1. Peschl P, Schanda K, Zeka B, et al. Human antibodies against the myelin oligodendrocyte glycoprotein can cause complement-dependent demyelination. *J Neuroinflammation*. 2017;14(1):208. doi:10.1186/s12974-017-0984-5